Supporting Information

Porous Monolith of Few-Layered Boron Nitride for Effective Water Cleanup

Chenyang Xu,[a] Jinjue Zeng,[a] Xianrui Gu,[b] Yue Wang,[a] Erchun Li,[a] Chen Zhang,[a] Cong Ge[a], Cheng Jin,[a] Meng Miao,[a] Zhu Jin,[a] Tian Gao,[a] Xiangfen Jiang,[c,d] Pengcheng Dai,[e] Yoshio Bando,[c,f,g] Ruiqing Li,[h] Junfeng Rong,[b] and Xue-Bin Wang[a]

[a.] National Laboratory of Solid State Microstructures (NLSSM), Collaborative Innovation Center of Advanced Microstructures, College of Engineering and Applied Sciences, Nanjing University, Nanjing, 210093, China

[b.] Research Institute of Petroleum Processing, SINOPEC, Beijing, 100083, China

[c.] International Center for Materials Nanoarchitectonics (MANA), National Institute for Materials Science (NIMS), Tsukuba, 3050044, Japan

[d.] Gotion Japan Co. Ltd., Tsukuba, 3050005, Japan

[e.] Institute of New Energy, State Key Laboratory of Heavy Oil Processing, China University of Petroleum (East China), Qingdao, 266580, China

[f.] Institute of Molecular Plus, Tianjin University, Tianjin, 300072, China

[g.] Australian Institute for Innovative Materials, University of Wollongong, North Wollongong, NSW 2500, Australia

[h.] School of Chemistry and Chemical Engineering, Liaocheng University, Liaocheng, 252059, China

Content

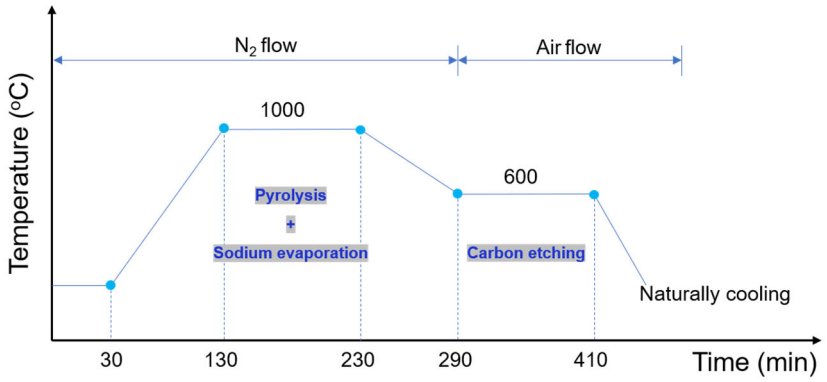

Fig. S1. Experimental program for borax-and-melamine pyrolysis for producing tcBN.

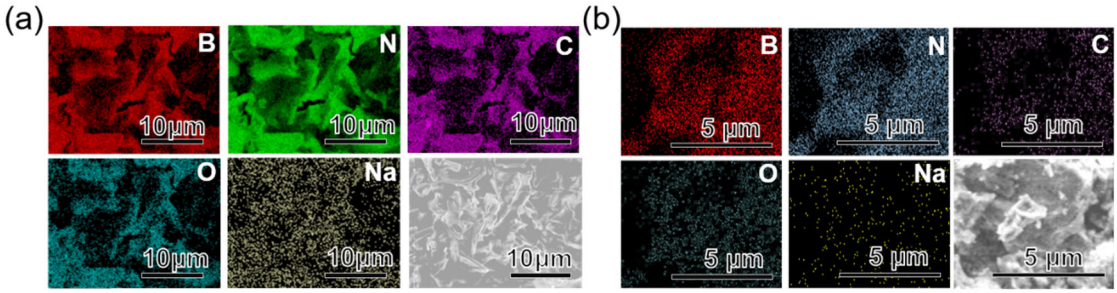

Fig. S2. EDS mappings of intermediate and tcBN. (a) EDS mapping of the intermediate, showing the existence of carbon element. (b) EDS mapping of tcBN. Boron and nitrogen elements emerge at the same place with similar atomic ratio, and they are far stronger than others, indicating the formation of BN.

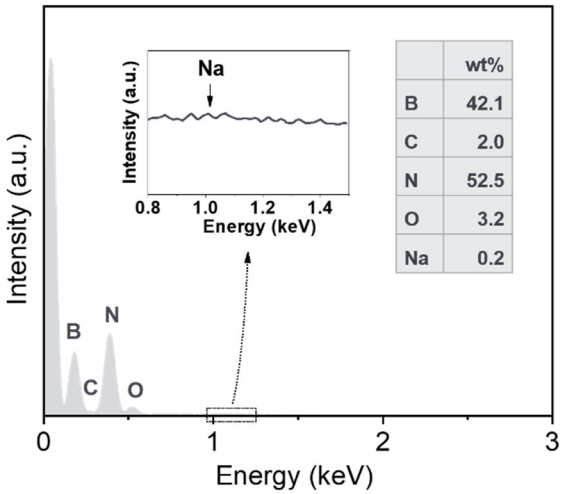

Fig. S3. EDS spectrum of tcBN. The atomic ratio of boron and nitrogen elements approaches 1:1. Other elements are fairly low.

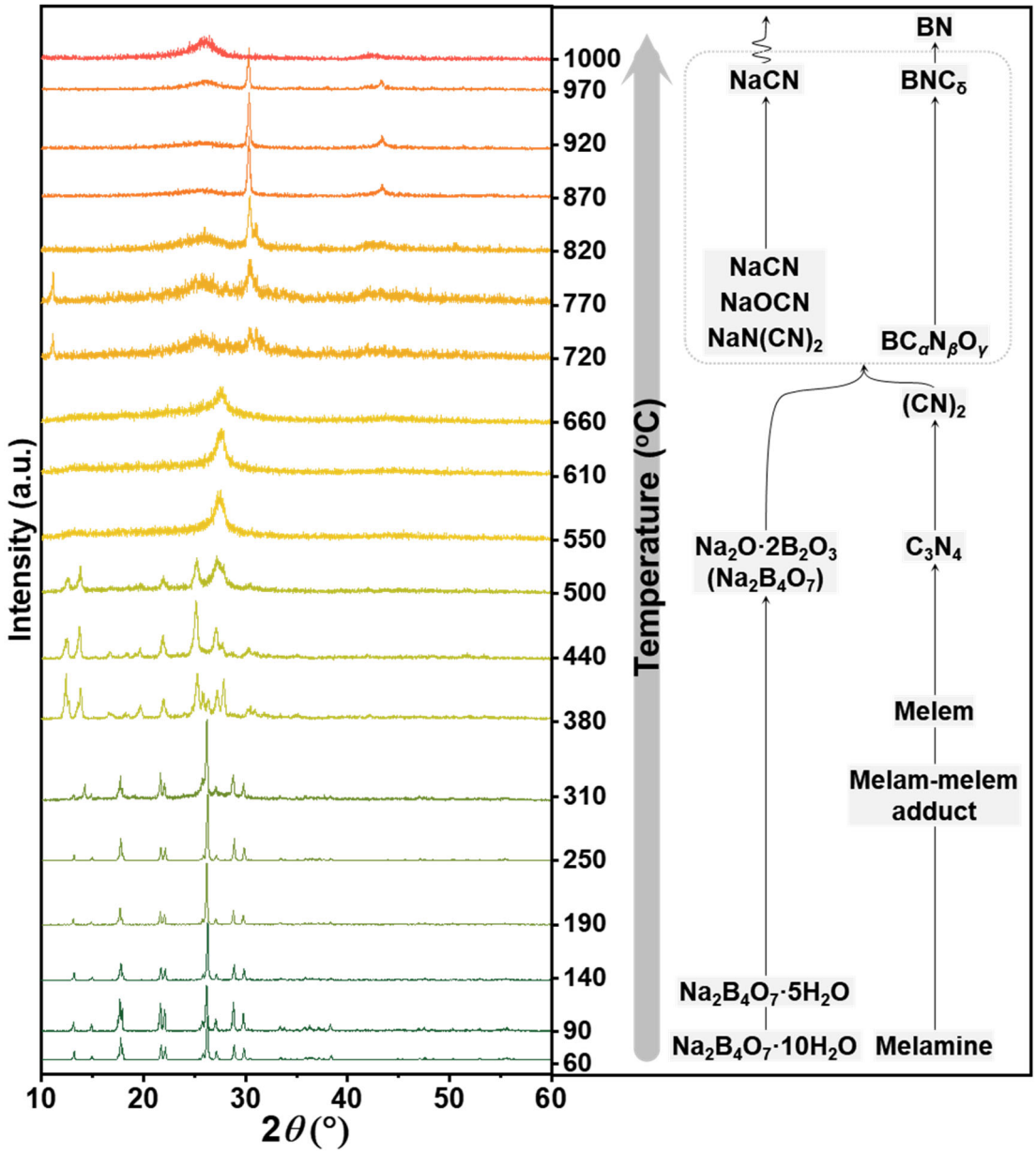

Fig. S4. XRD patterns of intermediates taken at marked temperatures during heating borax-and-melamine for synthesis of tcBN.

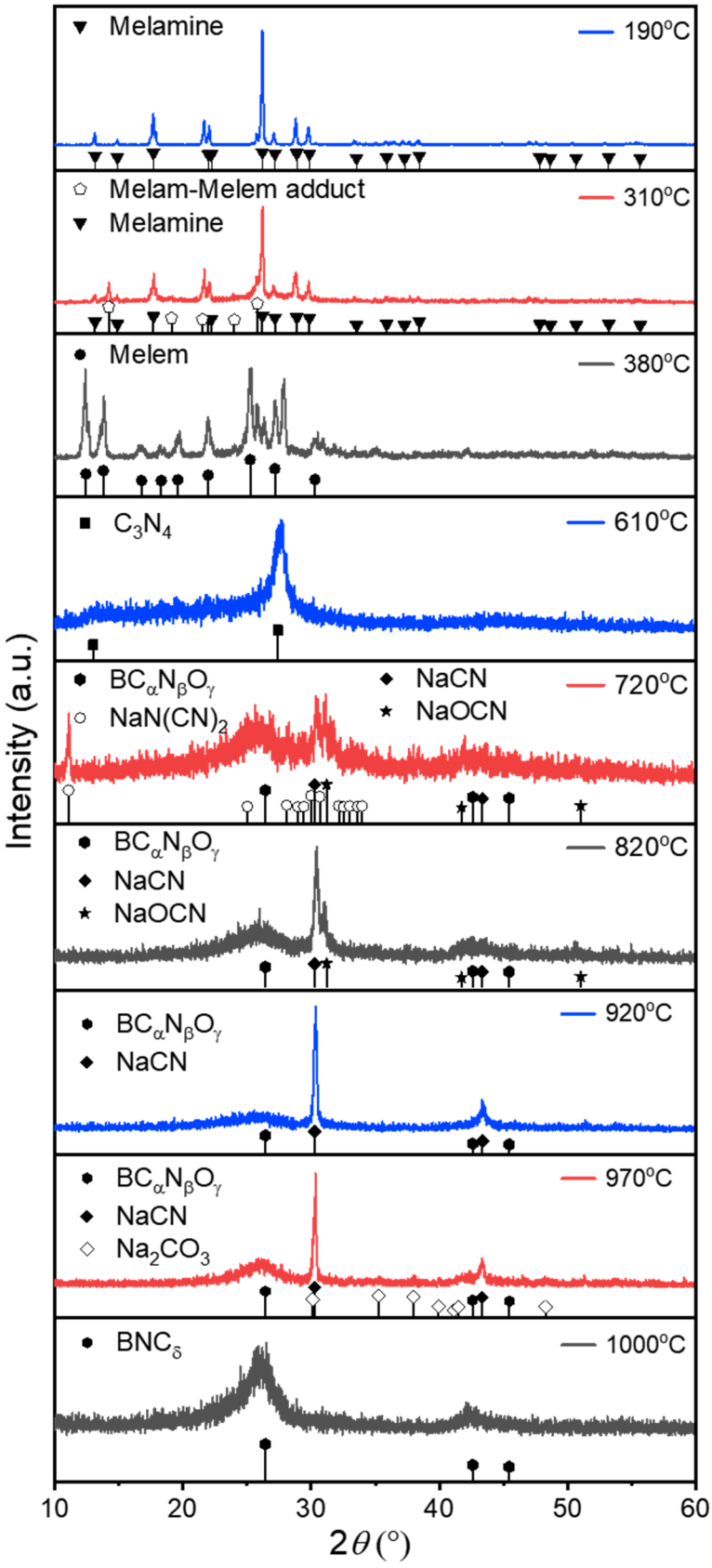

Fig. S5. Detailed XRD profiles of key intermediates taken at marked temperatures.

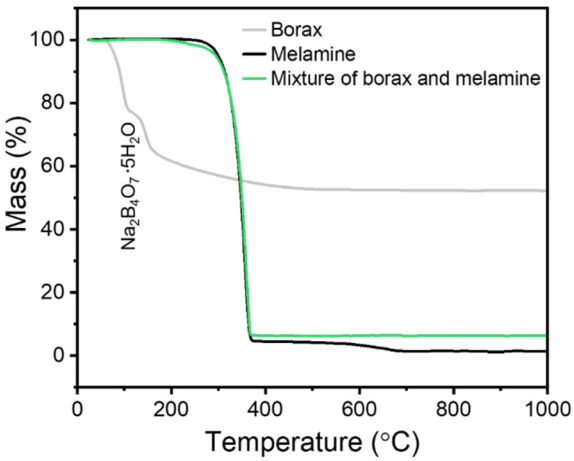

Fig. S6. TG curves of borax, melamine and borax-and-melamine precursor.

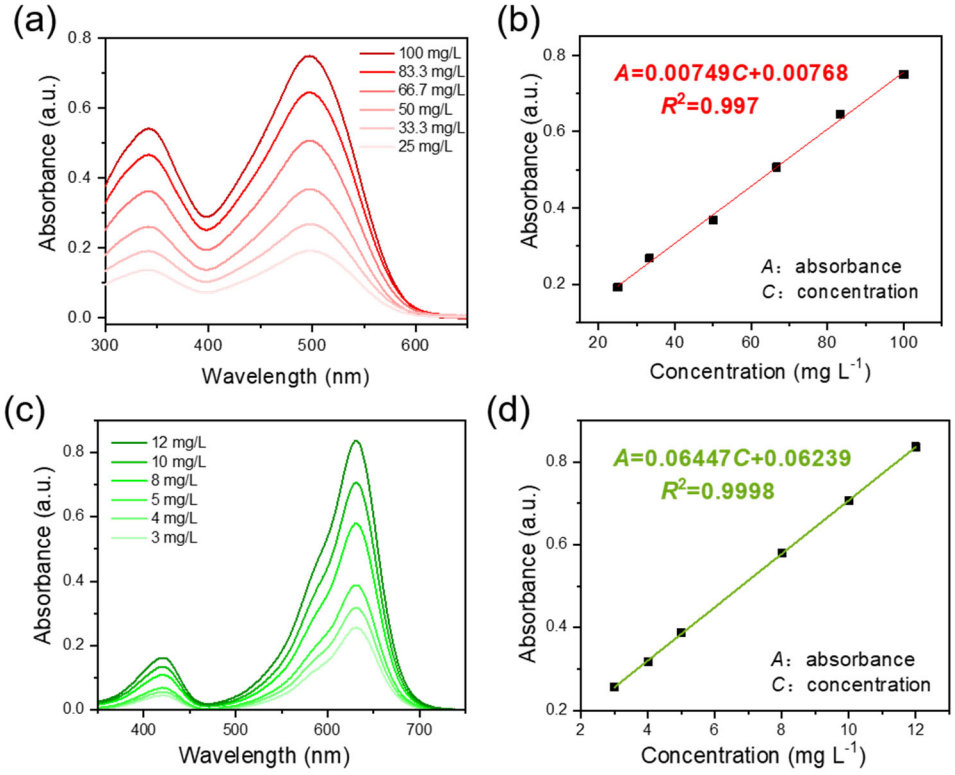

Fig. S7. Working curves of CR and MG standards for dye adsorption. (a,c) Absorbance curves of prepared CR and MG aqueous solutions, respectively. (b,d) Working curves fitted by the absorbance of CR and MG solutions at wavelengths of 496 nm and 632 nm, respectively.

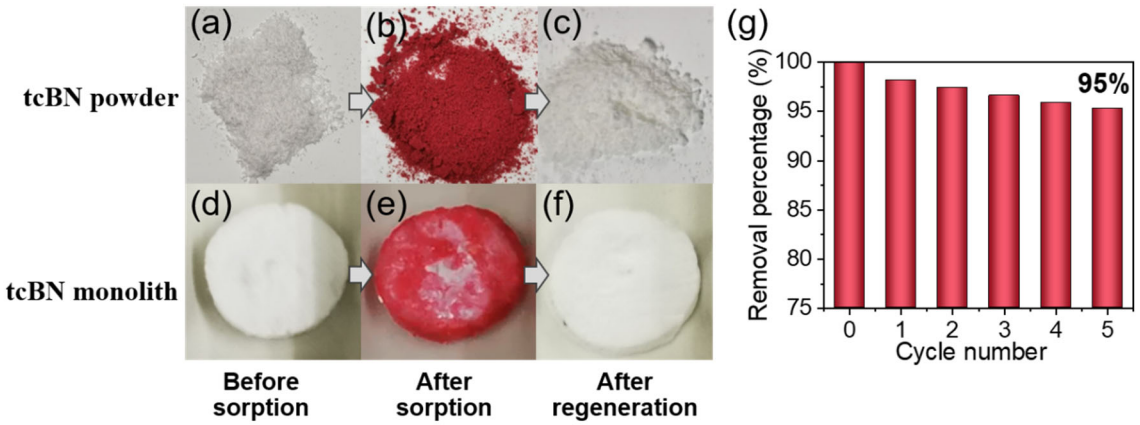

Fig. S8. Photos of tcBN powder and tcBN monolith, taken before sorption, after sorption and after regeneration *via* incineration. (a-c) tcBN powder for CR adsorption test. (d-g) tcBN monolith for oil absorption test.

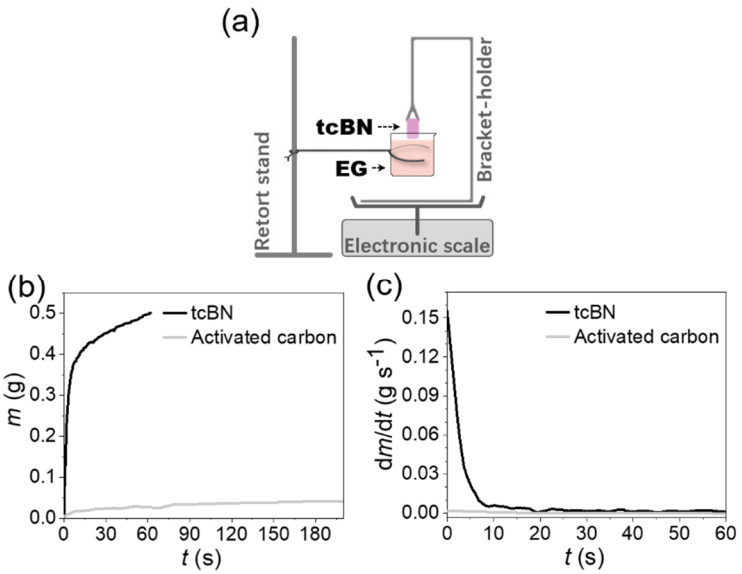

Fig. S9. Sorption kinetics of tcBN monolith on oil. (a) Sketch of the testing equipment. Ethylene glycol, EG, is used as a model adsorbate. (b) Accumulative weight of adsorbate absorbed within tcBN *vs* time. (c) Rate of weight gain of ethylene glycol absorbed within tcBN *vs* time.

In the kinetic test, a cylindric tcBN monolith is fixed to the rigid holder. Ethylene glycol in a beaker approaches slowly until the liquid level covers tcBN. The weight of the whole system is recorded in real time. The mass of adsorbate absorbed in tcBN, m, is calculated by the following formula equation,

$$m = m_t - m_0 \quad (1)$$

where m_t is the real-time mass, and m_0 is the mass at the moment of the sorbent soaking to the oil. Extensive researches have shown that the liquid sorption kinetics can be described by

"sharp-front capillary rise model". Considering gravity effect, the accumulative mass of absorbed adsorbate is a time-dependent equation,[1]

$$m_s = a[1 - \exp(-b\sqrt{t})] \quad (2)$$

where m_s symbolizes the accumulative mass of absorbed adsorbate *per* unit contact area, and a, b are coefficients relating with gravitational limiting sorption and sorptivity. At the beginning of time, equation (3) can reduce mathematically to be

$$m_s = K_s\sqrt{t} \quad (3)$$

where K_s is liquid sorption coefficient. It is further expressed as

$$K_s = \rho\frac{\varepsilon}{\tau}\sqrt{r\frac{\sigma}{\upsilon}\cos\frac{\theta}{2}} \quad (4)$$

where ρ, σ and υ represent density, surface tension and viscosity of adsorbate. ε and τ represent accessible porosity and pore tortuosity of sorbent, θ is the contact angle between liquid and sorbent. K_s is an important parameter popularly used in liquid sorption processes. It reflects the sorption speed of a sorbent on an adsorbate, regardless of gravity effect. K_s is gotten through fitting the linear region at the beginning of time. Specifically, tcBN has K_s of 0.35 kg m^{-2} $s^{-1/2}$, which indubitably indicates the excellent sorption speed of tcBN as compared with activated carbon (0.008 kg m^{-2} $s^{-1/2}$).

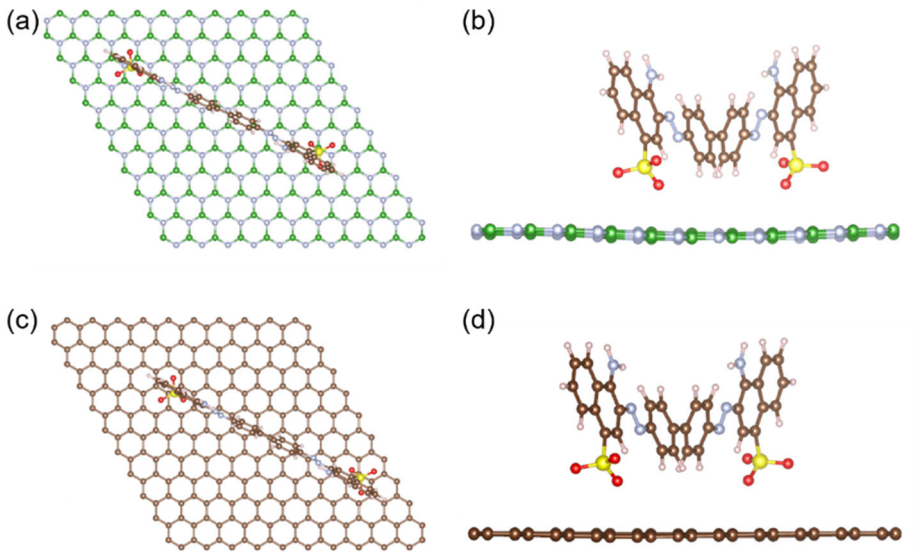

Fig. S10. Structure models of adsorption of Congo red on BN and graphene. (a,b) Top and side views of Congo red molecule on BN monolayer. (c,d) Congo red on graphene. The adsorption energy is defined as $E_{ads} = E_{con\text{-}sub} - E_{con} - E_{sub}$, where $E_{con\text{-}sub}$, E_{con} and E_{sub} stand for the calculated total energy of boron nitride or graphene substrate with Congo red, the isolated Congo red and the substrate, respectively.

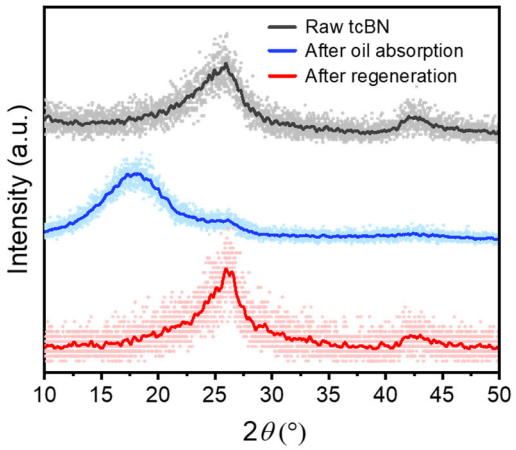

Fig. S11. XRD patterns of raw tcBN, tcBN after oil absorption and tcBN after regeneration.

Table S1. Detailed reaction mechanism of heating borax-and-melamine for synthesis of tcBN.

Temp. (°C)	Boron chemical evolution	Nitride chemical evolution	XRD	TG evidences
20-200	▪ Borax → $Na_2B_4O_7·5H_2O$	/	Melamine	▪ Borax loses 23wt% of initial mass at 120°C; It loses 47wt% at 500°C, *i.e.* all crystal water. ▪ Melamine loses most of initial mass at 380°C; It polymerizes into C_3N_4 at 550°C; C_3N_4 decomposes into cyanogen, cyano fragment, N_2 and tiny carbon at 700°C. * *J. Am. Chem. Soc.* 1926, 48, 695 ** *Metall. Mater. Trans. B.* 2001, 32B, 17
310-700	▪ $Na_2B_4O_7·5H_2O$ → $Na_2B_4O_7$ ▪ $Na_2B_4O_7$ is also $Na_2O·2B_2O_3$ ▪ B-rich and Na-rich phase segregation of Na-B-O system around 730°C	▪ Sublimation of melamine ▪ Melamine → Cyanamide ▪ Melamine → Melam + NH_3	Melam-melem adduct	
		▪ Melam → Melem + NH_3	Melem	
		▪ Melem → C_3N_4	C_3N_4	
700-820	▪ C_3N_4 → C + N_2 + $(CN)_2$ ▪ $Na_2O·2B_2O_3$ + NH_2CN → $NaN(CN)_2$ + $BC_\alpha N_\beta O_\gamma$ + CO + NH_3 ▪ 2 $Na_2O·2B_2O_3$ + (7+4α-4γ) $(CN)_2$ = 4 NaOCN + 8 $BC_\alpha N_\beta O_\gamma$ + (10-8γ) CO + (5+4α-4β-4γ) N_2		$BC_\alpha N_\beta O_\gamma$ $NaN(CN)_2$ NaOCN NaCN	
700-870	▪ NaCNO + $(CN)_2$ → NaCN + CO+ N_2 ▪ NaCNO → Na_2CO_3 + NaCN + CO+ N_2		$BC_\alpha N_\beta O_\gamma$ NaCN Na_2CO_3	
1000	▪ Sublimation of part of NaCN ▪ NaCN → Na_2C_2 ↑ + Na ↑ + C + N_2 ↑ * ▪ Na_2CO_3 + C → Na ↑ + CO ↑ ** ▪ $BC_\alpha N_\beta O_\gamma$ → BNC_δ + CO ↑		BNC_δ	

Table S2. Kinetic constants of adsorption *via* fitting the experimental dye adsorption from solution in Figure 5c, g. k_1 and k_2 are related kinetic parameters.

	Pseudo-first-order model		*Pseudo-second-order model*	
	k_1 (min^{-1})	R^2	k_2 (g mg^{-1} min^{-1})	R^2
Congo red	8.39×10^{-2}	0.953	4.39×10^{-4}	0.985
Methyl green	8.68×10^{-2}	0.975	4.16×10^{-4}	0.994

Table S3. Comparison of adsorption capacities of porous BN on Congo red.

Sample	*Synthesis category*	*Precursor*	*SSA* ($m^2\ g^{-1}$)	*Main pore type*	*Dye*	Q_m ($mg\ g^{-1}$)	*Ref.*
Porous BN	Non-templated method	Boron trioxide and guanidine hydrochloride	1427	Macropore Micropore	Congo red	782	[2]
3D BN	Non-templated method	Boron trioxide and urea	1156	Mesopore Micropore	Congo red	718	[3]
Flower stamen-like BN	Soft-templated method	Boric acid and urea with P123 as template	890	Micropore	Congo red	620	[4]
Cheese-like 3D C-BN	Hard-templated method	Boron acid and melamine with a template produced by boron oxide and triethanolamine	334	Mesopore	Congo red	307	[5]
Thin-wall cellular BN, tcBN	**Borax-melamine pyrolysis**	**Borax and melamine**	**1420**	**Mesopore**	**Congo red**	**1096**	**This work**

Movie S1. Absorption behavior of pump oil on water using tcBN monolith.

Movie S2. Oil/water separation in a home-made separator using tcBN as sieve.

Supporting references

1. M. Raimondo, M. Dondi, D. Gardini, G. Guarini and F. Mazzanti, *Constr. Build. Mater.* 2009, **23**, 2623.

2. W. W. Lei, D. Portehault, D. Liu, S. Qin and Y. Chen, *Nat. Commun.* 2013, **4**, 1377.

3. D. Liu, W. W. Lei, S. Qin and Y. Chen, *Sci. Rep.* 2014, **4**, 4453.

4. J. M. Wang, J. Hao, D. Liu, S. Qin, C. Chen, C. Yang, Y. C. Liu, T. Y. Yang, Y. Fan, Y. Chen and W. W. Lei, *Nanoscale* 2017, **9**, 9787.

5. Z. Y. Liu, Y. Fang, H. C. Jia, C. Wang, Q. Q. Song, L. L. Li, J. Lin, Y. Huang, C. Yu and C. C. Tang, *Sci. Rep.* 2018, **2**, 1104.